Current bounds and future prospects of light neutralino dark matter in the NMSSM

Rahool Barman

based on Phys. Rev. D **103**, 015029 (2021)

with Genevieve Belanger (LAPTh), Biplob Bhattacherjee (IISc), Rohini Godbole (IISc), Dipan Sengupta (Univ. of California), Xerxes Tata (Univ. of Hawaii)

HEP Weekly Seminar,
Oklahoma State University

February 4, 2021

Contents

- Why NMSSM?
- The Higgs and electroweakino sectors of NMSSM and implications from current constraints.
- Features of the allowed parameter space.
- Prospects at future experiments.

Introduction

- The ATLAS and CMS collaborations have unambiguously confirmed the existence of a scalar boson at 125 GeV.
- Numerous measurements by both, ATLAS and CMS, indicate that the properties of the observed resonance is consistent with the predictions from SM.
- The current data still leaves enough space for the observed Higgs to have non-standard decays.
- Higgs decaying to invisible particles provides one such exciting prospect.
- Invisible particles, if stable, could also be the dark matter candidate.
- Within R-parity conserved SUSY scenarios, the lightest stable particle, typically χ_1^0 (lightest neutralino), naturally provides a DM candidate.
- Correlations between invisible Higgs measurements, Dark Matter direct detection and direct/indirect collider probes, can provide interesting directions towards exploring the SUSY landscape.

Introduction

- Supersymmetry is an extended space-time symmetry which relates the fermionic and bosonic degrees of freedom:

$$Q_\alpha|fermion\rangle_\alpha = |boson\rangle, \quad Q_\alpha|boson\rangle = |fermion\rangle_\alpha \tag{1}$$

- The fermions and bosons related through Q_α are referred to as superpartners and grouped together under a supermultiplet.
- The supersymmetric extension of the Standard Model with the minimal field content in the Higgs sector is the Minimal Supersymmetric Standard Model (MSSM).
- The field content of the MSSM

	Supermultiplet	Fields	Spin	$SU(3)_C,\ SU(2)_L,\ U(1)_Y$
Quarks and Squarks	$\hat{Q}$	(u_L, d_L)	1/2	$(3,\ 2,\ 1/3)$
		$(\tilde{u}_L, \tilde{d}_L)$	0	
	$\hat{U}^C$	$\bar{u}_R$	1/2	$(\bar{3},\ 1,\ -4/3)$
		$\tilde{u}_R^*$	0	
	$\hat{D}^C$	$\bar{d}_R$	1/2	$(\bar{3},\ 1,\ 2/3)$
		$\tilde{d}_R^*$	0	
Leptons and Sleptons	$\hat{L}$	$(\nu_e,\ e_L)$	1/2	$(1,\ 2,\ -1)$
		$(\tilde{\nu}_e,\ \tilde{e}_L)$	0	
	$\hat{E}^C$	$\tilde{e}_R$	1/2	$(1,\ 1,\ 2)$
		$\tilde{e}_R^*$	0	

	Supermultiplet	Fields	Spin	$SU(3)_C,\ SU(2)_L,\ U(1)_Y$
Higgs and higgsinos	$\hat{H}_u$	$(H_u^+,\ H_u^0)$	0	$(1,\ 2,\ 1)$
		$(\tilde{H}_u^+,\ \tilde{H}_u^0)$	1/2	
	$\hat{H}_d$	$(H_d^0,\ H_d^-)$	0	$(1,\ 2,\ -1)$
		$(\tilde{H}_d^0,\ \tilde{H}_d^-)$	1/2	
B boson and Bino		B	1	$(1,\ 1,\ 0)$
		$\tilde{B}$	1/2	
W boson and Wino		$W^3,\ W^\pm$	1	$(1,\ 3,\ 1)$
		$\tilde{W}^3,\ \tilde{W}^\pm$	1/2	
Gluons and Gluinos		g	1	$(8, 1, 0)$
		$\tilde{g}$	1/2	

- The Higgs sector of MSSM features 5 Higgs bosons: 2 neutral scalars (H_1, H_2), 1 neutral pseudoscalar (A_1), and charged Higgses $(H^{\pm})$.

- The electroweakino sector:

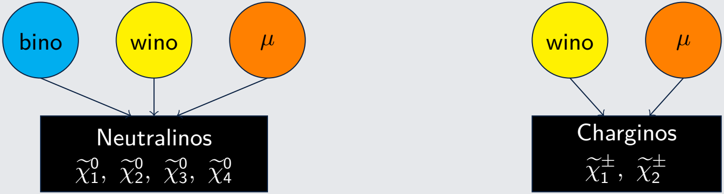

$\widetilde{\chi}_1^0$ can be a viable DM candidate if R-parity conservation is assumed.

- The MSSM has solved various issues with the Standard Model, however, it has its own problems.

Why NMSSM?

1. Solves the μ problem in MSSM: The NMSSM offers an elegant solution to the μ-problem in MSSM through the introduction of an additional singlet superfield ($\hat{S}$).

$$W_{MSSM} = y_u^{ij}\hat{u}_i\hat{Q}_j \cdot \hat{H}_u - y_d^{ij}\hat{d}_i\hat{Q}_j \cdot \hat{H}_d - y_e^{ij}\hat{E}_i\hat{L}_j \cdot \hat{H}_d + \boxed{\mu\hat{H}_u \cdot \hat{H}_d}$$

$$W_{NMSSM} = W_{MSSM}(\mu = 0) + \lambda\hat{S}\hat{H}_u \cdot \hat{H}_d + \frac{k}{3}\hat{S}^3$$

It naturally generates an effective μ term when S develops a non-zero vev $\langle S \rangle$.

2. Less tuning required for a 125 GeV SM-like Higgs boson:

$$M_{h_{SM}}^2 \sim M_Z^2 \cos^2 2\beta + \lambda^2 v^2 \sin^2 2\beta + \frac{3m_t^4}{4\pi^2 v^2}\left(ln\left(\frac{m_{stop}^2}{m_t^4}\right) + ...\right)$$

MSSM (Tree level): $M_h < M_Z \cdot |\cos 2\beta| \lesssim M_Z$
NMSSM (Tree level): $M_h^2 = M_Z^2 \cos^2 2\beta + \lambda^2 v^2 \sin^2 2\beta$

❶ Solves the μ problem in MSSM: The NMSSM offers an elegant solution to the μ-problem in MSSM through the introduction of an additional singlet superfield ($\hat{S}$).

$$W_{MSSM} = y_u^{ij}\hat{u}_i\hat{Q}_j \cdot \hat{H}_u - y_d^{ij}\hat{d}_i\hat{Q}_j \cdot \hat{H}_d - y_e^{ij}\hat{E}_i\hat{L}_j \cdot \hat{H}_d + \boxed{\mu\hat{H}_u \cdot \hat{H}_d}$$

$$W_{NMSSM} = W_{MSSM}(\mu = 0) + \boxed{\lambda\hat{S}\hat{H}_u \cdot \hat{H}_d} + \frac{k}{3}\hat{S}^3$$

It naturally generates an **effective μ term** ($\mu \sim \lambda\langle S\rangle$) when S develops a non-zero vev $\langle S\rangle$. NMSSM is the simplest SUSY extension of the SM in which the weak scale is generated by the SUSY breaking scale.

❷ Less tuning required for a 125 GeV SM-like Higgs boson:

$$M_{h_{SM}}^2 \sim M_Z^2\cos^2 2\beta + \lambda^2 v^2 \sin^2 2\beta + \frac{3m_t^4}{4\pi^2 v^2}\left(ln\left(\frac{m_{stop}^2}{m_t^4}\right) + ...\right)$$

MSSM (Tree level): $M_h < M_Z \cdot |\cos 2\beta| \lesssim M_Z$
NMSSM (Tree level): $M_h^2 = M_Z^2\cos^2 2\beta + \lambda^2 v^2 \sin^2 2\beta$

Why NMSSM?

1. Solves the μ problem in MSSM: The NMSSM offers an elegant solution to the μ-problem in MSSM through the introduction of an additional singlet superfield ($\hat{S}$).

$$W_{MSSM} = y_u^{ij}\hat{u}_i\hat{Q}_j \cdot \hat{H}_u - y_d^{ij}\hat{d}_i\hat{Q}_j \cdot \hat{H}_d - y_e^{ij}\hat{E}_i\hat{L}_j \cdot \hat{H}_d + \boxed{\mu\hat{H}_u \cdot \hat{H}_d}$$

$$W_{NMSSM} = W_{MSSM}(\mu = 0) + \lambda\hat{S}\hat{H}_u \cdot \hat{H}_d + \frac{k}{3}\hat{S}^3$$

It naturally generates an effective μ term when S develops a non-zero vev $\langle S \rangle$.

2. Less tuning required for a 125 GeV SM-like Higgs boson:

$$M_{h_{SM}}^2 \sim M_Z^2 \cos^2 2\beta + \boxed{\lambda^2 v^2 \sin^2 2\beta} + \frac{3m_t^4}{4\pi^2 v^2}\left(ln\left(\frac{m_{stop}^2}{m_t^4}\right) + ...\right)$$

MSSM (Tree level): $M_h < M_Z \cdot |\cos 2\beta| \lesssim M_Z$
NMSSM (Tree level): $M_h^2 = M_Z^2 \cos^2 2\beta + \lambda^2 v^2 \sin^2 2\beta$

Why NMSSM?

Richer Higgs sector

- 7 Higgs bosons: 3 neutral scalars (H_1, H_2, H_3), 2 neutral pseudoscalars (A_1, A_2), and charged Higgses ($H^{\pm}$)
  The scalars and pseudoscalars are an admixtures of doublets and singlet.

- Offers an exciting possibility to have light singlet-dominated a_1 and/or h_1 below 125 GeV (Ref. [12, 11, 22, 21, 23, 16]).
- Compared to MSSM, new terms $\propto \lambda, \kappa, v_s$ are introduced in the couplings of the Higgs with other Higgses and electroweakinos.
- Added complication: More input parameters are required to parametrize the tree level Higgs sector:

$$\lambda,\ \kappa,\ A_\lambda,\ A_\kappa,\ \tan\beta,\ \mu$$

Richer electroweakino sector

- 5 neutralinos (MSSM + singlino) and 2 charginos ($\widetilde{\chi}_1^{\pm}$, $\widetilde{\chi}_2^{\pm}$):

$$\chi_i^0 = N_{i1}\tilde{B} + N_{i2}\tilde{W}^3 + N_{i3}\tilde{H}_d^0 + N_{i4}\tilde{H}_u^0 + N_{i5}\tilde{S} \tag{2}$$

- At the tree level, the EW ino sector is parametrized by: M_1, M_2, $\mu, \tan\beta$, λ, κ.

The neutralino mass matrix at tree level:

$$M_{\chi_i^0} = \begin{pmatrix} M_1 & 0 & -M_Z \sin\theta_W \cos\beta & M_Z \sin\theta_W \sin\beta & 0 \\ 0 & M_2 & M_Z \cos\theta_W \cos\beta & -M_Z \cos\theta_W \sin\beta & 0 \\ -M_Z \sin\theta_W \cos\beta & M_Z \cos\theta_W \cos\beta & 0 & -\mu & \boxed{-\lambda v \sin\beta} \\ M_Z \sin\theta_W \sin\beta & -M_Z \cos\theta_W \sin\beta & -\mu & 0 & \boxed{-\lambda v \cos\beta} \\ 0 & 0 & \boxed{-\lambda v \sin\beta} & \boxed{-\lambda v \cos\beta} & \boxed{2\kappa v_s} \end{pmatrix}$$

- The singlino helps in alleviating constraints on neutralino dark matter.

Why NMSSM?

- In the MSSM with heavy sfermions, light neutralinos below $\sim 30\ \mathrm{GeV}$ are constrained [18, 5, 15, 9, 8, 7, 17, 4].
- This arises mainly from a combination of the relic density constraint and the chargino mass constraint.
- The NMSSM allows the possibility of a lighter neutralino ($O(1)$ GeV) while satisfying the upper limit on the relic density and other current constraints (Ref. [2, 10, 1, 19, 13, 3, 14]).
- The NMSSM also allows the possibility of light scalar and pseudoscalar Higgs bosons (below 125 GeV) which can escape the existing constraints from Higgs measurements.
- These singlet-dominated light Higgses provide an efficient annihilation mechanism for the light neutralinos in the early universe [6, 20].
- So, the NMSSM preserves the success of the MSSM while offering a multitude of additional possibilities.

- We choose the parameter space with:
  - $M_{\tilde{\chi}_1^0} < 62.5\ \mathrm{GeV}$
  - $\Omega h^2 \leq 0.120$
  - M_{h_1} and M_{a_1} below 122 GeV
- h_2 is identified with the SM-like Higgs boson.
- heavy squarks and sleptons to decouple their effects on the light neutralino sector.

The scan is performed over the following range of input parameters:

$$0.01 < \lambda < 0.7,\ 10^{-5} < \kappa < 0.05,\ 3 < \tan\beta < 40$$
$$100\ \mathrm{GeV} < \mu < 1\ \mathrm{TeV},\ 1.5\ \mathrm{TeV} < M_3 < 10\ \mathrm{TeV}$$
$$2\ \mathrm{TeV} < A_\lambda < 10.5\ \mathrm{TeV},\ -150\ \mathrm{GeV} < A_\kappa < 100\ \mathrm{GeV}$$
$$M_1 = 2\ \mathrm{TeV},\ 70\ \mathrm{GeV} < M_2 < 2\ \mathrm{TeV}$$
$$A_t = 2\ \mathrm{TeV},\ A_{b,\tilde{\tau}} = 0,\ M_{U_R^3}, M_{D_R^3}, M_{Q_L^3} = 2\ \mathrm{TeV},\ M_{e_L^3}, M_{e_R^3} = 3\ \mathrm{TeV}$$

Constraints

Limits from LEP:

- $M_{\widetilde{\chi}_1^\pm} \gtrsim 103.5$ GeV.
- Upper limits on $\sigma(e^+e^- \to \widetilde{\chi}_i^0 \widetilde{\chi}_1^0)$ at 95% CL.
- Upper limits from searches in $e^+e^- \to ZH_j/A_iH_j$

Flavor constraints:

- $3.00 \times 10^{-4} < Br(B \to X_s\gamma) < 3.64 \times 10^{-4}$.
- $1.73 \times 10^{-9} < Br(B_s \to \mu^+\mu^-) < 4.33 \times 10^{-9}$.
- $0.68 \times 10^{-4} < Br(B^+ \to \tau^+\nu_\tau) < 1.44 \times 10^{-4}$.

Limits from LHC

- Higgs signal strength constraints.
- Limits from sparticle searches at the LHC.
- Direct search of light Higgs bosons in the $2b2\tau$, $2b2\mu$ and $2\mu2\tau$ channels.
- $\Gamma_{h_{125}} < 22$ MeV
- $Br(h_{125} \to inv.) < 19\%$.

Constraints

Limits from LEP:

- $M_{\widetilde{\chi}_1^\pm} \gtrsim 103.5\ \mathrm{GeV}$.
- Upper limits on $\sigma(e^+e^- \to \widetilde{\chi}_i^0\widetilde{\chi}_1^0)$ at 95% CL.
- Upper limits from searches in $e^+e^- \to ZH_j/A_iH_j$

Flavor constraints:

- $3.00 \times 10^{-4} < Br(B \to X_s\gamma) < 3.64 \times 10^{-4}$.
- $1.73 \times 10^{-9} < Br(B_s \to \mu^+\mu^-) < 4.33 \times 10^{-9}$.
- $0.68 \times 10^{-4} < Br(B^+ \to \tau^+\nu_\tau) < 1.44 \times 10^{-4}$.

Limits from LHC

- Constraints from direct electroweakino searches
  - $pp \to (\chi_i^0 \to Z/h\chi_1)(\chi_1^\pm \to W^\pm\chi_1^0)$ resulting in $3l + E_{miss}^t$ final state. $\to$ Excludes a wino upto $\sim 600\ \mathrm{GeV}$ for $M_{\widetilde{\chi}_1^0} \lesssim 60\ \mathrm{GeV}$.
  - Direct chargino pair-production in OS di-lepton$+\not{E}_\mathrm{T}$ final state $\to$ excludes wino-like $\widetilde{\chi}_1^\pm$ below $\lesssim 400\ \mathrm{GeV}$ for bino-like $M_{\widetilde{\chi}_1^0} \sim 50\ \mathrm{GeV}$.

Constraints from direct detection:

- The blue and orange points are allowed by the latest upper limits on σ_{SI} from Xenon-1T.
- Blue points are further excluded by the latest UL's on σ_{SD} $\rightarrow$ these points feature a large $N_{13}^2 - N_{14}^2$.

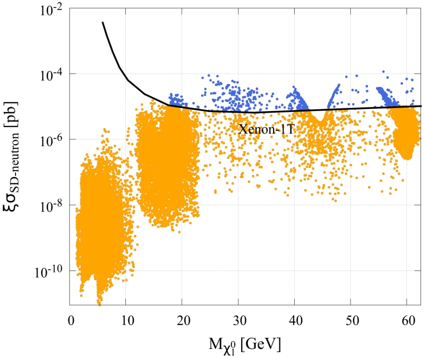

Indirect detection constraints:

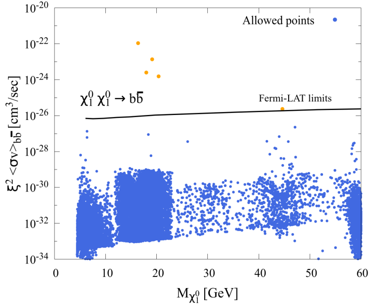

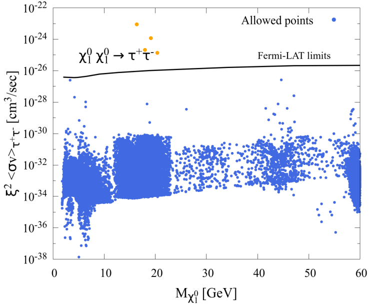

- A small number of points shown in orange are excluded.

- Grey: Excluded by LEP limits, Higgs signal strength constraints, B-physics constraints, direct light Higgs searches and sparticle searches at the LHC.
- Green: excluded by direct detection.
- Orange: excluded by direct electroweakino searches.

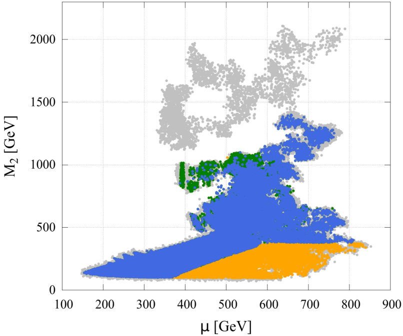

- The large M_2 region is mostly excluded by the Higgs signal strength constraints and LEP searches for light Higgs.
- The impact of Higgs constraints could be relaxed in a more generic framework where the parameters of the squark sector are also allowed to vary.

What's different from MSSM?

The allowed region in MSSM:

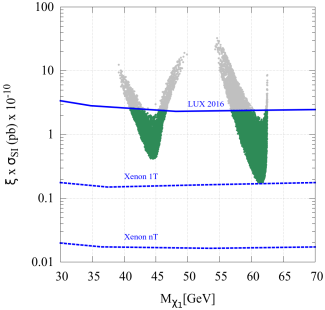

from 1703.03838

- The lower bound on $M_{\tilde{\chi}_1^0}$ implies the presence of only Z and h_{125} as mediators for the efficient $\tilde{\chi}_1^0\tilde{\chi}_1^0$ annihilation.
- The NMSSM, on the other hand, features additional singlet-like h_1 and a_1 below M_Z $\rightarrow$ possible to obtain allowed points in NMSSM with $M_{\tilde{\chi}_1^0} \sim 1$ GeV.

- Below 62.5 GeV, the $\widetilde{\chi}_1^0$ has to be bino or singlino dominated.
- $\Omega h^2 \leq 0.122$ can be satisfied only through co-annihilation or annihilation via resonance.
- For our parameter space, co-annihilation $\longrightarrow$ $\boxed{\textit{not feasible}}$
- Only possibility $\rightarrow$ annihilation via resonance.
- We fix M_1 at 2 TeV $\rightarrow$ $\widetilde{\chi}_1^0$ is always singlino dominated.
- The singlino-like $\widetilde{\chi}_1^0$ below $M_Z/2$ can undergo annihilation through a_1 or h_1.
- To evade the current constraints, light a_1 and h_1 must be singlet dominated.

- Below the Z funnel region:
  1. the allowed points are mostly populated along $M_{a_1} \sim 2M_{\widetilde{\chi}_1^0}$.
  2. points away from the above correlation have $M_{h_1} \sim 2M_{\widetilde{\chi}_1^0}$.

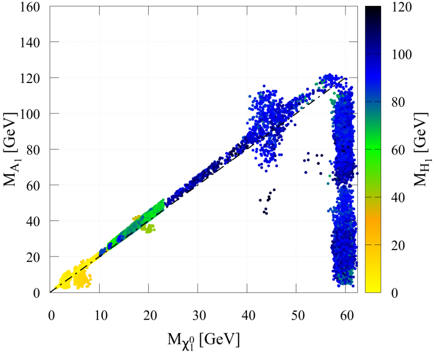

Complementarity between future direct detection experiments and invisible Higgs measurements

Black points: $Br(H_{125} \to inv.) < 0.24\% \to$ outside the projected Higgs invisible measurement capability of CEPC.

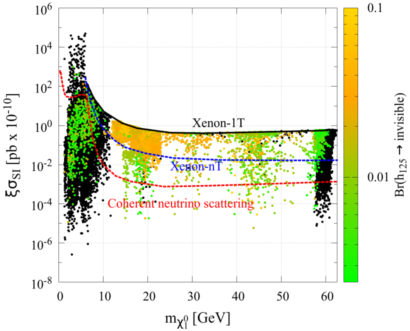

- CEPC will be able to probe the green colored points in the $M_{\tilde{\chi}_1^0} \lesssim 10$ GeV region which may be forever outside the reach of DM detectors.
- CEPC will also be able to probe points which are outside Xenon-nT's future reach.

Complementarity between future direct detection experiments and invisible Higgs measurements

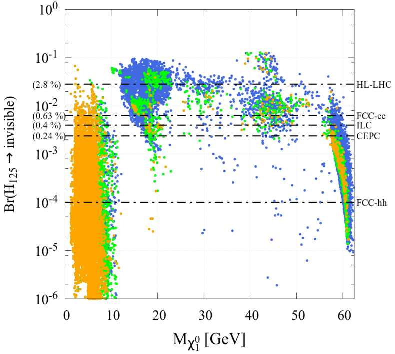

HL−LHC ($\gtrsim$ 2.8%) [CMS-PAS-FTR-16-002],
FCC−ee ($\gtrsim$ 0.63%) [1605.00100],
ILC ($\gtrsim$ 0.4%) [1310.0763],
CEPC ($\gtrsim$ 0.24%) [1811.10545],
FCC−hh ($\gtrsim$ 0.01%) [CERN-ACC-2018-045]

- Orange: points below the coherent neutrino scattering floor.
- Green: points outside Xenon-nT's projected reach but above the neutrino scattering floor.

Additional coverage with future σ_{SD} measurements

- The spin-dependent measurements can provide coverage of some parameter space points with small σ_{SI} (even below the coherent neutrino scattering floor).
- Roughly similar to the `blind spots` $\rightarrow$ very small value of σ_{SI} while also being compatible with relic density limits.

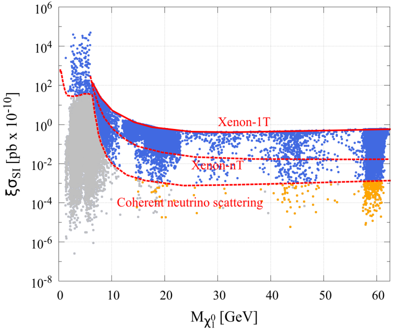

Projected reach of future light Higgs searches

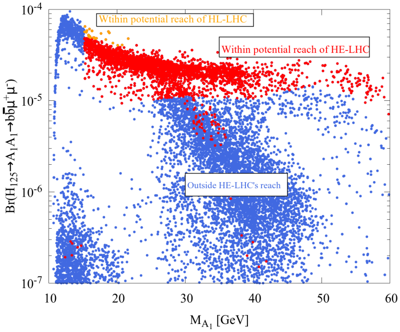

The future projections have been taken from 1902.00134 and translated to our allowed parameter space.

- Blue colored points: Outside the projected reach of direct light Higgs searches in the $pp \to h_{125} \to a_1 a_1/h_1 h_1 \to 2b2\mu$ channel.
- The results indicate that the discovery potential of light Higgs bosons produced via direct decays of H_{125} is not very strong.
- We made no attempt to optimize the analysis for increased luminosity or increased energy. So, our conclusion must be viewed with caution.

- Next, the projected reach of direct electroweakino searches (in WZ and Wh_{125} mediated $3l + \not{E}_T$ channel) at the HL-LHC and the HE-LHC is derived through cut-based collider analysis using optimized signal regions.
- A simplified model with degenerate higgsino-like $\widetilde{\chi}_3^0, \widetilde{\chi}_2^0, \widetilde{\chi}_1^\pm$ and bino-like $\widetilde{\chi}_1^0$ is considered while evaluating the projections.
- The goal is to map out how well the future upgrades of LHC will be able to probe the NMSSM parameter space with light neutralino.
- The projections are translated to the allowed NMSSM parameter space by considering the actual production cross-sections and branching ratios of the mixed states.
- In order to do so, the signal efficiency grids are mapped out in the doublet-higgsino LSP mass plane.
- Since the efficiency grid is determined by the kinematics, the details of the composition of the parent higgsinos or the daughter LSP is completely irrelevant. Thus, the projections could be potentially translated to any model parameter space.

Signal: $pp \to \widetilde{\chi}_2^0 \widetilde{\chi}_1^\pm \to WZ + \not{E}_T \to 3l + \not{E}_T$.
Backgrounds: WZ, $t\bar{t}Z$, VVV, ZZ.

Signal regions:

	Benchmark points							
	BPA1	BPB1	BPC1	BPD1	BPE1	BPF1	BPG1	BPH1
$M_{\widetilde{\chi}_2^0, \widetilde{\chi}_3^0, \widetilde{\chi}_1^\pm}$ [GeV]	130	310	310	610	610	610	1000	1000
$M_{\widetilde{\chi}_1^0}$ [GeV]	30	0	210	0	300	510	0	420
Kinematic variables	Signal regions							
	SRA1	SRB1	SRC1	SRD1	SRE1	SRF1	SRG1	SRH1
$\Delta\Phi_{l_W \not{E}_T}$	≤ 0.2	-	≤ 1.5	-	-	-	-	-
$\Delta\Phi_{SFOS-\not{E}_T}$	-	$[2.7 : \pi]$	$[1.8 : \pi]$	$[1.5 : \pi]$	$[1.8 : \pi]$	-	$[1.6 : \pi]$	$[1.5 : \pi]$
ΔR_{SFOS}	[1.4 : 3.8]	[0.3 : 2.1]	-	[0.1 : 1.3]	[0.1 : 1.3]	[1.6 : 4.0]	[0.1 : 1.0]	[0.1 : 1.3]
$\not{E}_T$ [GeV]	[50 : 290]	≥ 220	[100 : 380]	≥ 200	≥ 250	-	≥ 200	≥ 200
$M_T^{l_W}$ [GeV]	-	≥ 100	[100 : 225]	≥ 300	≥ 150	[150 : 350]	≥ 150	≥ 200
$M_{CT}^{l_W}$ [GeV]	-	≥ 100	-	≥ 100	≥ 150	[100 : 400]	≥ 200	≥ 200
$p_T^{l_1}$ [GeV]	[50 : 150]	≥ 120	[60 : 110]	≥ 150	≥ 150	[60 : 150]	≥ 210	≥ 200
$p_T^{l_2}$ [GeV]	[50 : 110]	≥ 60	≥ 30	≥ 100	≥ 100	[50 : 80]	≥ 150	≥ 100
$p_T^{l_3}$ [GeV]	≥ 30	≥ 30	≥ 30	≥ 50	≥ 50	[30 : 60]	≥ 50	≥ 50

Background generation (at LO) done using MadGraph5_aMC@NLO. Signal generated using Pythia-6 and detector effects simulated with Delphes-3.4.2.

Efficiency maps:

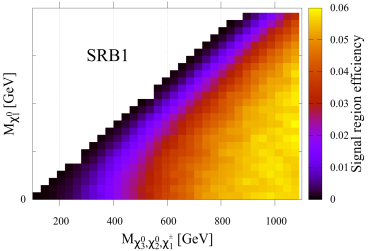

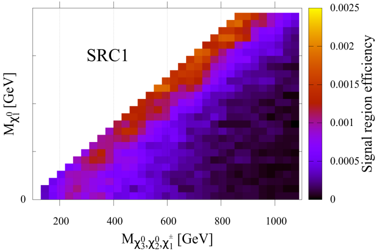

Projected reach of wino searches in the WZ mediated $3l + \not{E}_T$ final state at the HL-LHC.

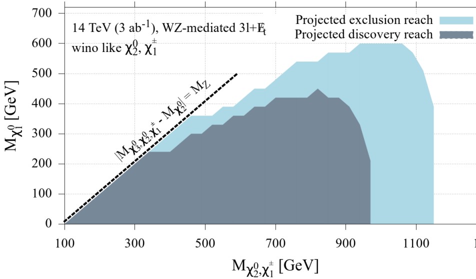

Our projection results are comparable with the ATLAS projections in ATL-PHYS-PUB-2018-048 (discovery (exclusion) upto $\sim$950 ($\sim$ 1110) GeV for massless LSP at 95% C.L.).

WZ-mediated $3l + \not{E}_T$ at the HL-LHC

Projected reach of wino searches in the WZ mediated $3l + \not{E}_T$ final state at the HL-LHC.

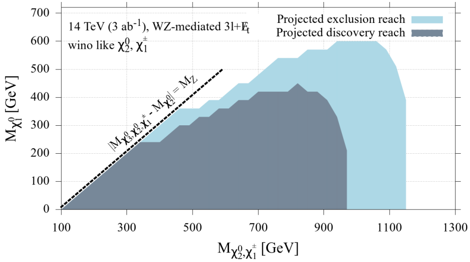

Our projection results are comparable with the ATLAS projections in ATL-PHYS-PUB-2018-048 (discovery (exclusion) upto $\sim$950 ($\sim$ 1110) GeV for massless LSP at 95% C.L.).

Projected reach of higgsino searches in the WZ mediated $3l + \not{E}_T$ final state at the HL-LHC.

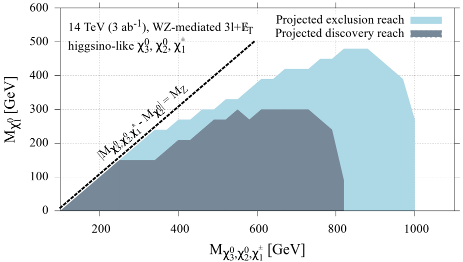

A systematic uncertainty of 5% has been assumed in these analyses.

- In our allowed parameter region, $\widetilde{\chi}_2^0, \widetilde{\chi}_3^0, \widetilde{\chi}_4^0, \widetilde{\chi}_1^{\pm}, \widetilde{\chi}_2^{\pm}$ are either higgsino-like, wino-like or wino-higgsino admixtures.
- Direct chargino-neutralino pair production modes which can potentially contribute to WZ mediated $3l + \not{E}_{\mathrm{T}}$: $\widetilde{\chi}_2^0\widetilde{\chi}_1^{\pm}$, $\widetilde{\chi}_2^0\widetilde{\chi}_2^{\pm}$, $\widetilde{\chi}_3^0\widetilde{\chi}_1^{\pm}$, $\widetilde{\chi}_3^0\widetilde{\chi}_2^{\pm}$, $\widetilde{\chi}_4^0\widetilde{\chi}_1^{\pm}$ and $\widetilde{\chi}_4^0\widetilde{\chi}_2^{\pm}$
- The direct production cross-section ($\sigma_{\widetilde{\chi}_i^0\widetilde{\chi}_j^{\pm}}$) is computed by scaling the pure higgsino cross-section with the respective reduced squared $W\widetilde{\chi}_i^0\widetilde{\chi}_j^{\pm}$ couplings:

$$C^2_{W\widetilde{\chi}_i^0\widetilde{\chi}_j^{\pm}} = \left\{ \left(N_{i3}\ V_{j2} - N_{i2}\ V_{j1}\sqrt{2}\right)^2 + \left(N_{i4}\ U_{j2} + N_{i2}\ U_{j1}\sqrt{2}\right)^2 \right\}$$

U/V are the chargino mixing matrices while N represents the neutralino mixing matrix.

- The signal yield for a particular parameter space point is computed for all the signal regions through:

$$S = \sigma_{\widetilde{\chi}_i^0\widetilde{\chi}_j^{\pm}} \times (\mathit{Relevant\ Br\ ratios}) \times (\mathcal{L} = 3000\ \mathrm{fb}^{-1}) \times \mathit{Signal\ efficiency} \tag{3}$$

- The signal efficiency is obtained from the efficiency maps shown earlier.
- The signal significance (S_σ) is computed as: $S/\sqrt{B + (B \cdot sys\_un)^2}$, by adopting the signal region that yields the highest S_σ. Here, B stands for background.

Color code: Green: $S_\sigma > 5$, light blue: $2 < S_\sigma < 5$, dark blue: $S_\sigma < 2$

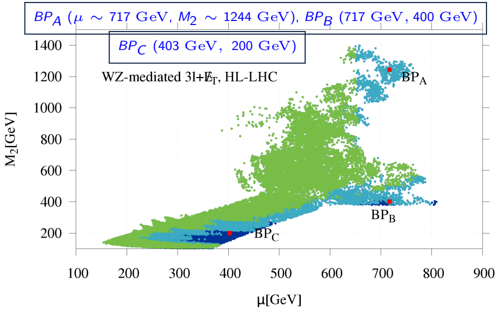

- The observation of a signal is an interplay between the production cross-section and signal efficiency.
- At large values of M_2, μ (near BP_A) $\rightarrow$ large efficiency but smaller production cross-section $\rightarrow$ kinematically suppressed signal.
- At smaller values of M_2, μ, $\rightarrow$ larger production cross-section but signal efficiencies reduce.
- The dark blue points near $BP_C \rightarrow S_\sigma$ marginally less than 2σ.
- In BP_B and BP_C, the dominant production mode is $\widetilde{\chi}_2^0 \widetilde{\chi}_1^\pm$, and $\widetilde{\chi}_2^0$ dominantly decays into $H_{125} + \widetilde{\chi}_1^0$ with branching rates of 82% and 92%, respectively $\rightarrow$ reduced sensitivity in WZ mediated channels.
- Direct searches in WH_{125} mediated channels could be more effective for these benchmarks.

Signal: $pp \to \widetilde{\chi}_2^0/\widetilde{\chi}_3^0 + \widetilde{\chi}_1^\pm \to Wh_{125} + \not{E}_T \to 3\mathrm{l} + \not{E}_T$
Main backgrounds: WZ, $t\bar{t}V$, VVV and ZZ

Signal regions:

Kinematic variables	Signal regions			
	SRA2	SRB2	SRC2	SRD2
$M_{OS,min}^{inv}$ [GeV]	< 75			
$\not{E}_T$ [GeV]	> 100			
$M_T^{l_1}$ [GeV]	≥ 200	≥ 200	≥ 300	≥ 400
$M_T^{l_2}$ [GeV]	≥ 100	≥ 150	≥ 200	≥ 150
$M_T^{l_3}$ [GeV]	≥ 100	≥ 100	≥ 150	≥ 100

These SRs are motivated from a similar analysis in ATL-PHYS-PUB-2014-010

Projected exclusion and discovery reach at the HL-LHC.

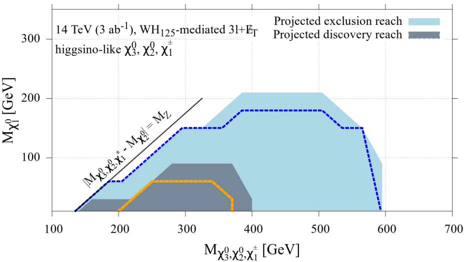

The projected reach on the currently allowed parameter space:

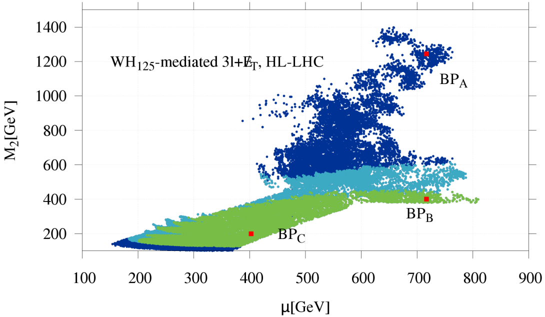

Direct searches in the WH_{125} mediated $3l + \not{E}_T$ channel are more effective in probing the $M_2 \lesssim \mu$ region of parameter space.

- BP_B and BP_C: outside the reach of direct searches in WZ mediated $3l + \not{E}_T$, but fall within the discovery reach of direct searches in the WH_{125} mediated channel.
- Similarly, the $M_2 \lesssim 150$ GeV region in this figure shows 5σ sensitivity via the WZ mediated $3l + \not{E}_T$ search channel.
- We observe a striking complementarity in the search power via WZ and WH_{125} mediated $3l + \not{E}_T$ search channels..

	$\widetilde{\chi}_1^0$	$\widetilde{\chi}_2^0$	$\widetilde{\chi}_3^0$	$\widetilde{\chi}_4^0$	$\widetilde{\chi}_1^\pm$	$\widetilde{\chi}_2^\pm$
Mass [GeV]	60.4	421	734	742	421	741
wino %	10^{-5}	0.96	2×10^{-3}	0.04	0.94	0.06
higgsino %	10^{-4}	0.04	0.99	0.96	0.06	0.94
Singlino fraction in $\widetilde{\chi}_1^0$: 0.99			$M_{H_1}=97.2$ GeV, $M_{A_1}=99$ GeV			
Cross-section (fb)	$\widetilde{\chi}_2^0\widetilde{\chi}_1^\pm$	$\widetilde{\chi}_2^0\widetilde{\chi}_2^\pm$	$\widetilde{\chi}_3^0\widetilde{\chi}_1^\pm$	$\widetilde{\chi}_3^0\widetilde{\chi}_2^\pm$	$\widetilde{\chi}_4^0\widetilde{\chi}_1^\pm$	$\widetilde{\chi}_4^0\widetilde{\chi}_2^\pm$
$\sqrt{s}=14$ TeV	104	0.27	0.28	2.1	0.25	2.3
$\sqrt{s}=27$ TeV	363	1.1	1.1	10.2	1.0	11.2
Branching ratio	$\widetilde{\chi}_2^0\to\widetilde{\chi}_1^0 Z$ (0.04), $\widetilde{\chi}_1^0 H_{125}$ (0.82), $\widetilde{\chi}_1^0 H_1$ (0.14)					
	$\widetilde{\chi}_3^0\to\widetilde{\chi}_1^0 Z$ (0.13), $\widetilde{\chi}_1^0 H_{125}$ (0.10), $\widetilde{\chi}_1^0 H_1$ (0.01), $\widetilde{\chi}_1^\pm W^\mp$ (0.51), $\widetilde{\chi}_2^0 Z$ (0.23), $\widetilde{\chi}_2^0 H_{125}$ (0.01)					
	$\widetilde{\chi}_4^0\to\widetilde{\chi}_1^0 Z$ (0.12), $\widetilde{\chi}_1^0 H_{125}$ (0.11), $\widetilde{\chi}_1^\pm W^\mp$ (0.53) $\widetilde{\chi}_4^0\to\widetilde{\chi}_2^0 Z$ (0.02), $\widetilde{\chi}_2^0 H_{125}$ (0.21)					
Significance at HL-LHC: WZ mediated $3l+\cancel{E}_T$: 1.5, WH_{125} mediated $3l+\cancel{E}_T$: 5.3 Significance at HE-LHC: WZ mediated $3l+\cancel{E}_T$: 4.4, WH_{125} mediated $3l+\cancel{E}_T$: 34						

- Notice the presence of other cascade decay modes:
  1. $\widetilde{\chi}_3^0$ can decay into $\widetilde{\chi}_2^0 Z$, while $\widetilde{\chi}_2^0$ can decay into $\widetilde{\chi}_1^0 H_1$ or $\widetilde{\chi}_1^0 H_{125}$.
  2. $\widetilde{\chi}_3^0$ is dominantly produced in association with $\widetilde{\chi}_2^\pm$, which can decay into $Z/H_{125}+\widetilde{\chi}_1^\pm$ or $W^\pm+\widetilde{\chi}_2^0/\widetilde{\chi}_1^0$ with appreciable rates.
  3. $\widetilde{\chi}_3^0\widetilde{\chi}_2^\pm$ can eventually lead to rich final states including $VV+\cancel{E}_T$ or $V/Z/H_1+\cancel{E}_T$. Although, $\sigma(\widetilde{\chi}_3^0\widetilde{\chi}_2^\pm)$ is small for BP_B, but one obtain points with relatively larger $\sigma(\widetilde{\chi}_3^0\widetilde{\chi}_2^\pm)$, for. eg. BP_C with $\sigma(\widetilde{\chi}_3^0\widetilde{\chi}_2^\pm)\sim 24.8$ fb.
- $3l+\cancel{E}_T$ channels might not be most the efficient ones in the presence of these cascade decay channels.
- Dedicated searches beyond the scope of this work will be needed to explore these novel signals.

Color code: Grey: projected discovery region, light blue: projected exclusion region

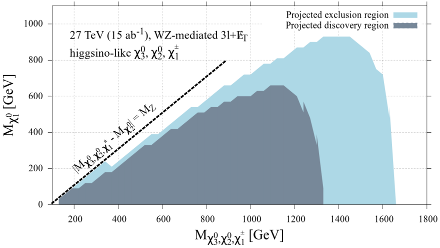

- We optimize 7 different signal regions to perform this search.
- Projected exclusion reach at the HL-LHC was only up to ~ 600 GeV.

- 10 optimized signal regions are considered.
- Considerable improvement over its HL-LHC counterpart. Projected exclusion reach at the HL-LHC was only up to ~ 1000 GeV for massless $\widetilde{\chi}_1^0$.

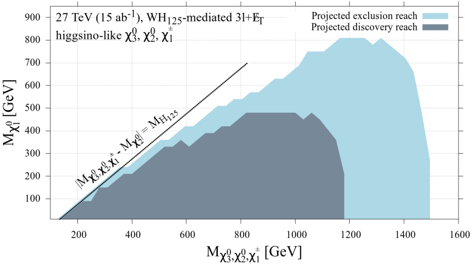

Color code: Green: $S_\sigma > 5$, light blue: $2 < S_\sigma < 5$, dark blue: $S_\sigma < 2$

WZ-mediated $3l + \not\!\!E_T$ channel

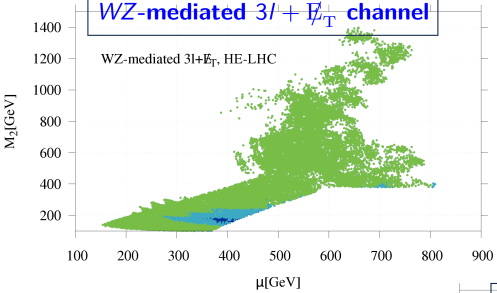

The HE-LHC provides a larger discovery opportunity than the HL-LHC for the detection of NMSSM inos with light LSP.

WH_{125}-mediated $3l + \not\!\!E_T$ channel

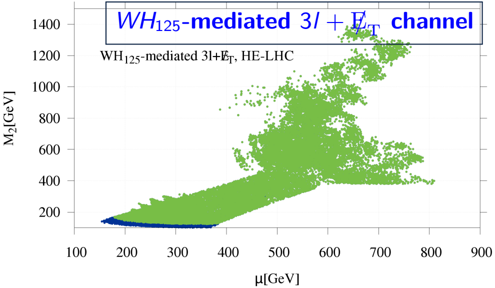

Combination of EW ino searches in the WZ and WH_{125} mediated $3l + \not\!\!E_T$ channel will probe all the currently allowed parameter space points at discovery potential.

We see a considerable improvement in the signal significance at the high energy upgrade of the LHC.

Benchmark point (M_2, μ) [in GeV]	WZ mediated		WH_{125} mediated	
	HL-LHC	HE-LHC	HL-LHC	HE-LHC
BP_A (1244, 717)	13 (3.8)	180 (14)	4 (0.4)	23 (6.6)
BP_B (400, 717)	7 (1.5)	86 (4.4)	63 (5.3)	272 (34)
BP_C (200, 403)	7 (1.3)	65 (2.1)	131 (8.8)	388 (48)
BP_D (952, 585)	20 (6.1)	231 (18)	8 (1.0)	35 (9.8)
BP_E (696, 518)	23 (7.0)	408 (20)	12 (1.2)	36 (10)
BP_F (555, 571)	28 (8.6)	418 (21)	18 (2.1)	79 (22)
BP_G (396, 515)	23 (5.2)	233 (12)	78 (5.3)	206 (27)
BP_H (204, 302)	17 (3.4)	167 (5.3)	125 (8.4)	368 (45)
BP_I (210, 262)	27 (5.3)	257 (8.1)	110 (7.4)	321 (40)

Conclusion

- The allowed parameter space features both a singlino-dominated LSP $\widetilde{\chi}_1^0$ and singlet-like light Higgs.
- DD experiments and Higgs invisible width measurements at the future experiments have the potential to cover some of the parameter space, however, the $M_{\widetilde{\chi}_1^0} \lesssim 10\ \mathrm{GeV}$ region will remain out of reach.
- The low mass region will also be out of the future reach of searches for light Higgses in SM-like Higgs decay.
- The Wh_{125} mediated EWino search channel was truly complementary in the $M_2 < \mu$ region where the WZ channel had the least power.
- Direct EWino searches at the HL-LHC would be able to discover a majority of currently allowed parameter space via at least one of the two channels.
- HE-LHC guarantees discovery via both WZ and Wh_{125} mediated $3l + \not{E}_{\mathrm{T}}$ channels over essentially the entire parameter space.

Thank you

Backup slides

Benchmark points	Input parameters
BP_A	$\lambda = 0.3$, $\kappa = 0.01$, $\tan\beta = 9.5$, $A_\lambda = 6687$ GeV, $A_\kappa = 5.2$ GeV, $\mu = 717$ GeV, $M_2 = 1244$ GeV, $M_3 = 2301$ GeV
BP_B	$\lambda = 0.44$, $\kappa = 0.02$, $\tan\beta = 11.8$, $A_\lambda = 8894$ GeV, $A_\kappa =$ -57 GeV, $\mu = 717$ GeV, $M_2 = 400$ GeV, $M_3 = 4323$ GeV
BP_C	$\lambda = 0.08$, $\kappa = 3 \times 10^{-4}$, $\tan\beta = 18$, $A_\lambda = 6563$ GeV, $A_\kappa =$ -7.9 GeV, $\mu = 403$ GeV, $M_2 = 200$ GeV $M_3 = 3080$ GeV
BP_D	$\lambda = 0.44$, $\kappa = 0.02$, $\tan\beta = 15.6$, $A_\lambda = 585$ GeV, $A_\kappa = 9501$ GeV, $\mu = 585$ GeV, $M_2 = 952$ GeV, $M_3 = 4457$ GeV
BP_E	$\lambda = 0.27$, $\kappa = 0.02$, $\tan\beta = 11.6$, $A_\lambda = 5875$ GeV, $A_\kappa = 12$ GeV, $\mu = 518$ GeV, $M_2 = 696$ GeV, $M_3 = 3634$ GeV
BP_F	$\lambda = 0.30$, $\kappa = 0.01$, $\tan\beta = 11.2$, $A_\lambda = 6319$ GeV, $A_\kappa = 17$ GeV, $\mu = 571$ GeV, $M_2 = 555$ GeV, $M_3 = 2687$ GeV
BP_G	$\lambda = 0.42$, $\kappa = 0.02$, $\tan\beta = 15.9$, $A_\lambda = 8638$ GeV, $A_\kappa = 43.4$ GeV, $\mu = 515$ GeV, $M_2 = 396$ GeV, $M_3 = 2903$ GeV
BP_H	$\lambda = 0.02$, $\kappa = 7 \times 10^{-5}$, $\tan\beta = 25.5$, $A_\lambda = 7348$ GeV, $A_\kappa =$ -7.3 GeV, $\mu = 302$ GeV, $M_2 = 204$ GeV, $M_3 = 2239$ GeV
BP_I	$\lambda = 0.02$, $\kappa = 6 \times 10^{-5}$, $\tan\beta = 27.6$, $A_\lambda = 6924$ GeV, $A_\kappa =$ -5.7 GeV, $\mu = 262$ GeV, $M_2 = 210$ GeV, $M_3 = 2217$ GeV

1. Implications from current constraints

The allowed parameter space

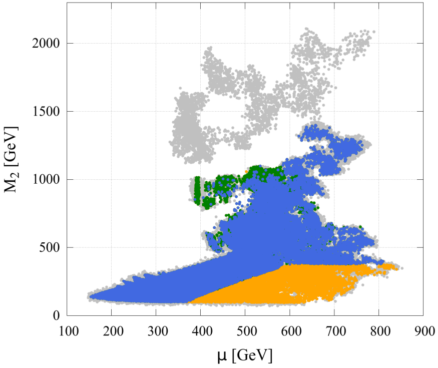

- Blue color: The allowed parameter space points.
- The grey and green points also lie beneath the blue and yellow colored points.

- Grey points: excluded by the constraints from: LEP, Higgs signal strength, *B* physics, direct light Higgs searches and sparticle searches at the LHC.
- Green and yellow regions: excluded by the SI direct detection limits from Xe-1T and the limits from direct EW ino searches in the $3l + \not{E}_T$ and $2l + \not{E}_T$ channels, respectively.
- The points in the large M_2 region are mostly excluded by the Higgs signal strength constraints, requirement of a 125 GeV Higgs and LEP searches for light Higgs.

We see a considerable improvement in the signal yields at the high energy upgrade of the LHC.

Benchmark point (M_2, μ) [in GeV]	WZ mediated		WH_{125} mediated	
	HL-LHC	HE-LHC	HL-LHC	HE-LHC
BP_A (1244, 717)	13 (3.8)	180 (14)	4 (0.4)	23 (6.6)
BP_B (400, 717)	7 (1.5)	86 (4.4)	63 (5.3)	272 (34)
BP_C (200, 403)	7 (1.3)	65 (2.1)	131 (8.8)	388 (48)
BP_D (952, 585)	20 (6.1)	231 (18)	8 (1.0)	35 (9.8)
BP_E (696, 518)	23 (7.0)	408 (20)	12 (1.2)	36 (10)
BP_F (555, 571)	28 (8.6)	418 (21)	18 (2.1)	79 (22)
BP_G (396, 515)	23 (5.2)	233 (12)	78 (5.3)	206 (27)
BP_H (204, 302)	17 (3.4)	167 (5.3)	125 (8.4)	368 (45)
BP_I (210, 262)	27 (5.3)	257 (8.1)	110 (7.4)	321 (40)

The numbers in represents the signal significance values.

Complementarity between future direct detection experiments and invisible Higgs measurements

Black points: $Br(H_{125} \to invisible) < 0.24\% \to$ outside the projected Higgs invisible measurement capability of CEPC.

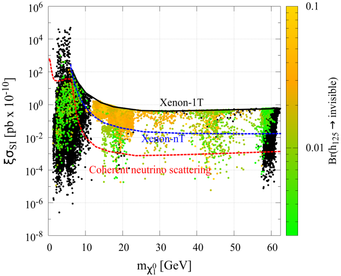

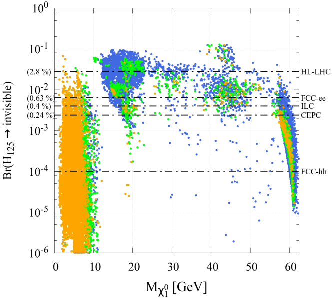

- CEPC will be able to probe the green colored points in the $M_{\tilde{\chi}_1^0} \lesssim 10$ GeV region which may be forever outside the reach of DM detectors.
- CEPC will also be able to probe points

- Orange: points below the coherent neutrino scattering floor.
- Green: points outside Xenon-nT's projected reach but above the neutrino scattering floor.

References I

D. Albornoz Vasquez, G. Belanger, and C. Boehm.
Astrophysical limits on light NMSSM neutralinos.
Phys. Rev., D84:095008, 2011.

D. Albornoz Vasquez, G. Belanger, C. Boehm, A. Pukhov, and J. Silk.
Can neutralinos in the MSSM and NMSSM scenarios still be light?
Phys. Rev., D82:115027, 2010.

D. Barducci, G. Belanger, C. Hugonie, and A. Pukhov.
Status and prospects of the nMSSM after LHC Run-1.
JHEP, 01:050, 2016.

R. K. Barman, G. Belanger, B. Bhattacherjee, R. Godbole, G. Mendiratta, and D. Sengupta.
Invisible decay of the Higgs boson in the context of a thermal and nonthermal relic in MSSM.
Phys. Rev., D95(9):095018, 2017.

G. Belanger, F. Boudjema, A. Cottrant, A. Pukhov, and S. Rosier-Lees.
Lower limit on the neutralino mass in the general MSSM.
JHEP, 03:012, 2004.

G. Belanger, F. Boudjema, C. Hugonie, A. Pukhov, and A. Semenov.
Relic density of dark matter in the NMSSM.
JCAP, 0509:001, 2005.

G. Belanger, G. Drieu La Rochelle, B. Dumont, R. M. Godbole, S. Kraml, and S. Kulkarni.
LHC constraints on light neutralino dark matter in the MSSM.
Phys. Lett., B726:773–780, 2013.

C. Boehm, P. S. B. Dev, A. Mazumdar, and E. Pukartas.
Naturalness of Light Neutralino Dark Matter in pMSSM after LHC, XENON100 and Planck Data.
JHEP, 06:113, 2013.

References II

L. Calibbi, T. Ota, and Y. Takanishi.
Light Neutralino in the MSSM: a playground for dark matter, flavor physics and collider experiments.
JHEP, 07:013, 2011.

J.-J. Cao, K.-i. Hikasa, W. Wang, J. M. Yang, K.-i. Hikasa, W.-Y. Wang, and J. M. Yang.
Light dark matter in NMSSM and implication on Higgs phenomenology.
Phys. Lett., B703:292–297, 2011.

D. G. Cerdeno, P. Ghosh, and C. B. Park.
Probing the two light Higgs scenario in the NMSSM with a low-mass pseudoscalar.
JHEP, 06:031, 2013.

F. Domingo, U. Ellwanger, E. Fullana, C. Hugonie, and M.-A. Sanchis-Lozano.
Radiative Upsilon decays and a light pseudoscalar Higgs in the NMSSM.
JHEP, 01:061, 2009.

U. Ellwanger and C. Hugonie.
The semi-constrained NMSSM satisfying bounds from the LHC, LUX and Planck.
JHEP, 08:046, 2014.

U. Ellwanger and C. Hugonie.
The higgsinoâĂŞsinglino sector of the NMSSM: combined constraints from dark matter and the LHC.
Eur. Phys. J., C78(9):735, 2018.

D. Feldman, Z. Liu, and P. Nath.
Low Mass Neutralino Dark Matter in the MSSM with Constraints from $B_s \to \mu^+\mu^-$ and Higgs Search Limits.
Phys. Rev., D81:117701, 2010.

M. Guchait and A. Roy.
Light Singlino Dark Matter at the LHC.
5 2020.

References III

K. Hamaguchi and K. Ishikawa.
Prospects for Higgs- and Z-resonant Neutralino Dark Matter.
Phys. Rev., D93(5):055009, 2016.

D. Hooper and T. Plehn.
Supersymmetric dark matter: How light can the LSP be?
Phys. Lett., B562:18–27, 2003.

J. Kozaczuk and S. Profumo.
Light NMSSM neutralino dark matter in the wake of CDMS II and a 126 GeV Higgs boson.
Phys. Rev., D89(9):095012, 2014.

F. Mahmoudi, J. Rathsman, O. Stal, and L. Zeune.
Light Higgs bosons in phenomenological NMSSM.
Eur. Phys. J., C71:1608, 2011.

A. M. Sirunyan et al.
Search for an exotic decay of the Higgs boson to a pair of light pseudoscalars in the final state of two muons and two τ leptons in proton-proton collisions at $\sqrt{s} = 13$ TeV.
JHEP, 11:018, 2018.

A. M. Sirunyan et al.
Search for an exotic decay of the Higgs boson to a pair of light pseudoscalars in the final state with two b quarks and two τ leptons in proton-proton collisions at $\sqrt{s} = 13$ TeV.
Phys. Lett., B785:462, 2018.

K. Wang and J. Zhu.
Funnel annihilations of light dark matter and the invisible decay of the Higgs boson.
Phys. Rev. D, 101:095028, 2020.